Journal of New Materials for Electrochemical Systems 19, 51-55 (2016)

Electrode Properties of Todorokite-type Tunnel-structured Manganese Oxide for Calcium Secondary Batteries

Shinya Suzuki*, Tsubasa Kato, Hidetoshi Kawabata and Masaru Miyayama

School of Engineering, The University of Tokyo,
7-3-1 Hongo, Bunkyo-ku, Tokyo 113-8656, Japan

Received: March 6, 2016, Accepted: April 12, 2016, Available online: July 02, 2016

Abstract: *The electrode properties of todorokite-type tunnel-structured manganese oxides (TodMO) were examined for their potential use as cathode materials in calcium batteries. TodMO with a chemical composition of $Mg_{0.19}Na_{0.07}MnO_2$ $0.37H_2O$ was prepared through hydrothermal treatment of layer-structured manganese oxide using magnesium ions as interlayer guest ions. The TodMO exhibited a discharge and charge capacity of 100 and 80 mAh g^{-1}, respectively, at a relatively large current density of 100 mA g^{-1}. The reaction mechanism was studied in detail using X-ray absorption spectroscopy measurements. Consequently, it became clear that the newly formed Mn^{3+}-compound converted from TodMO is responsible for the reversible capacity.*

Keywords: todorokite-type manganese oxide, cathodes, Ca batteries, X-ray absorption spectroscopy

1. INTRODUCTION

Li-ion rechargeable batteries have significant advantages over other batteries, and are widely used as energy-storage instruments in various mobile electric devices and electric vehicles. However, battery systems with higher energy densities are in considerable demand, and post-Li-ion batteries, for example, metal-air secondary batteries [1,2] and secondary batteries using naturally abundant s-block metals as anodes [3-7], are attracting an increasing amount of attention. In particular, the theoretical volumetric capacities of Mg, Ca, and Al are 3830, 2070, and 8050 mAh cm^{-3}, respectively; values that are larger than that of Li metal (2060 mAh cm^{-3}), because of the multi-electron reactions that occur within these materials. The anode behavior of Mg has been widely investigated [8], and an Mg electrolyte solution that enables reversible deposition and dissolution has previously been reported [9].

In addition, cathode materials using polyvalent cations as carriers have also been studied. Generally speaking, insertion reactions are preferable to conversion reactions for the electrode materials used in secondary batteries as regards cycling durability and coulombic efficiency. Although insertion electrode materials for polyvalent cations have primarily been investigated [5], only a small number of candidates (e.g., chevrel-phase Mo_6S_8 [4, 10]) have been found to date. This is mainly because of the low diffusivity of polyvalent cations in the solid phase, which is caused by strong electrostatic interactions between the guest cations and host structure.

We previously reported on tunnel-structured manganese oxide as an electrode for use in Mg batteries, based on the characteristic that magnesium ions can move through tunnels rapidly [11-13]. Specifically, it was found that a fine carbon composite of hollandite-type tunnel-structured manganese oxide exhibited a capacity of 140 mAh g^{-1} at a current density of 100 mA g^{-1}, which is relatively large for a Mg battery [11]. Hence, we supposed that the tunnel has the potential to act as a rapid diffusion path for calcium ions. In this study, the electrode properties of tunnel-structured manganese oxide were examined, with a view to implementation in Ca batteries. A todorokite-type manganese oxide (TodMO) with a [3 × 3] tunnel structure was adopted as the electrode material. The reaction mechanism of the TodMO in a Ca electrolyte solution was then evaluated in detail using X-ray absorption spectroscopy analyses.

2. EXPERIMENTAL

TodMO hydrate powders were prepared according to the meth-

*To whom correspondence should be addressed:
Department of Applied Chemistry, School of Engineering, The University of Tokyo,
7-3-1 Hongo, Bunkyo-ku, Tokyo 113-8656, Japan
Tel: +81-3-5841-7462, Fax: +81-3-5841-7462
E-mail: sin@fmat.t.u-tokyo.ac.jp

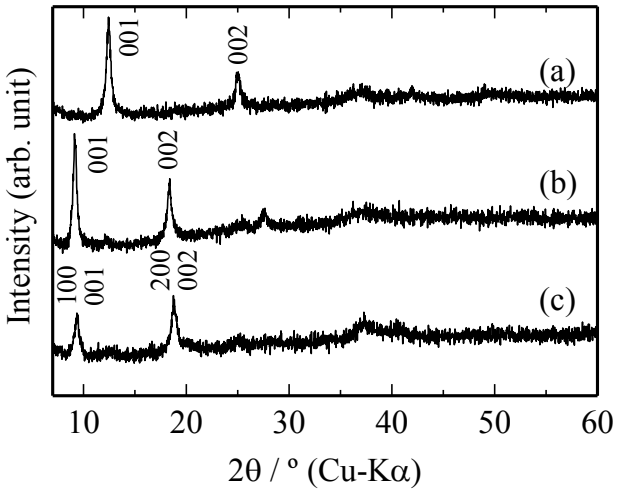

Figure 1. X-ray diffraction patterns of (a) birnessite-type sodium manganese oxide, (b) buserite-type magnesium manganese oxide, and (c) TodMO.

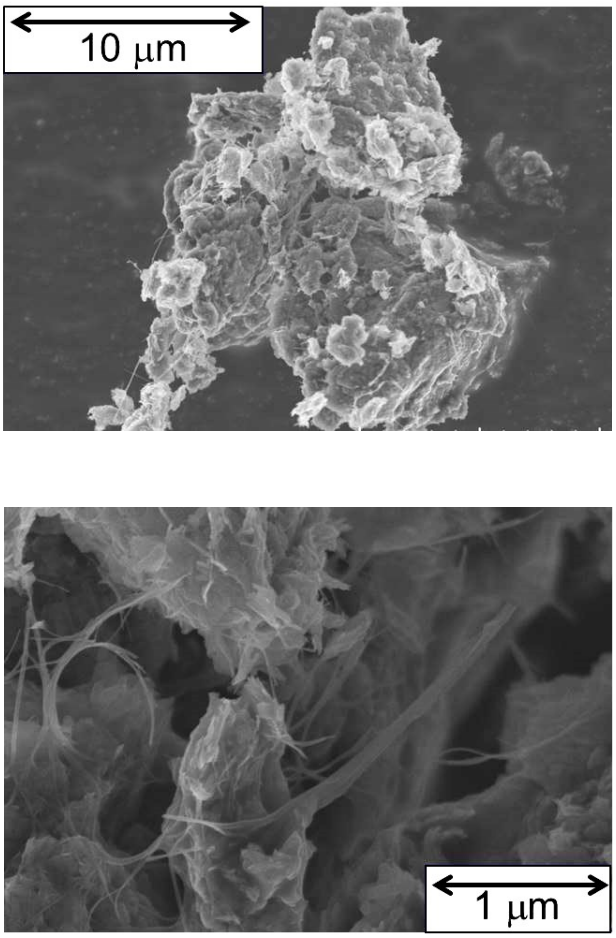

Figure 2. Scanning electron micrograph of obtained TodMO.

ods given in the previous literature [14]. Manganese hydroxide was first obtained by mixing a 0.1-mol dm^{-3} aqueous solution of $MnSO_4$ and a 5-mol dm^{-3} NaOH solution. A layer-structured birnessite-type sodium manganese oxide was obtained through immediate oxidation of the manganese hydroxide using a H_2O_2 solution under vigorous stirring, followed by aging for 12 h. A layer-structured buserite-type magnesium manganese oxide hydrate was prepared through ion-exchange from sodium to magnesium ions by dispersing the sodium manganese oxide in a 1-mol dm^{-3} $MgCl_2$ aqueous solution for 48 h at room temperature. The $MgCl_2$ solution was changed daily. TodMO was obtained through hydrothermal treatment of the buserite-type magnesium manganese oxide at 170 °C for 72 h in the 1-mol dm^{-3} $MgCl_2$ aqueous solution, followed by washing and drying.

The electrodes for the experimental measurements were prepared by pressing a mixture of TodMO hydrates, acetylene black (as a conducting additive), and polytetrafluoroethylene (as a binder) onto a Ti mesh. The weight ratio of the TodMO:carbon:binder was 45:45:10. The electrochemical properties of the TodMO powders in the non-aqueous calcium electrolyte solution were examined using the prepared electrodes as working electrodes. Two counter electrodes were used here, concidering the irreversible reactivity of Ca metal in a non-aqueous electrolyte solution [15]. One electrode featured Ca metal pressed onto the Ti mesh to yield electrochemical reduction of the working electrode, while the other was composed of large amount of V_2O_5 electrode [16] pressed onto the Ti mesh to yield electrochemical oxidation. As a reference electrode, silver wire was placed into an acetonitrile solution of 0.01-mol dm^{-3} $AgNO_3$ and 0.1-mol dm^{-3} tetrabutylammonium perchlorate. Beaker-type cells with four electrodes were fabricated using 0.2-mol dm^{-3} $Ca[(CF_3SO_2)_2N]_2$ in acetonitrile solution, as an electrolyte solution under an Ar atmosphere. All measurements were conducted at 20°C. Constant current charge/discharge tests were conducted within a potential range of -1.8–1.0 V (vs. Ag/Ag^+) using a Bio-Logic VMP3 potentiostat/galvanostat.

Ex situ X-ray absorption spectroscopy (XAS) measurements for the TodMO were conducted at the Mn K- or $L_{2,3}$-edges, both before and after the electrochemical measurements. The XAS measurements conducted at the Mn K-edge were performed using a transmission method at the BL-7C beamline at the KEK Photon Factory (KEK-PF), and those at the $L_{2,3}$-edge were conducted using the total electron yield mode of the BL-2 beamline at the SR Center of Ritsumeikan University.

3. RESULTS AND DISCUSSION

Figure 1 shows the X-ray diffraction patterns of the fabricated (a) birnessite-type sodium manganese oxide, (b) buserite-type magnesium manganese oxide, and (c) TodMO. Ion-exchange from sodium to magnesium ions within the layered compound caused an increase in the basal spacing. The slight changes in the peak position and strongest peak between (b) and (c) indicate the transformation from a layered structure to a [3 × 3] tunnel structure.

Figures 2(a) and 2(b) are scanning electron micrographs of the obtained TodMO. Aggregation was observed, which was composed of plate-like particles and a small amount of fibrous particles. In previous reports, two forms of TodMO were observed, and the

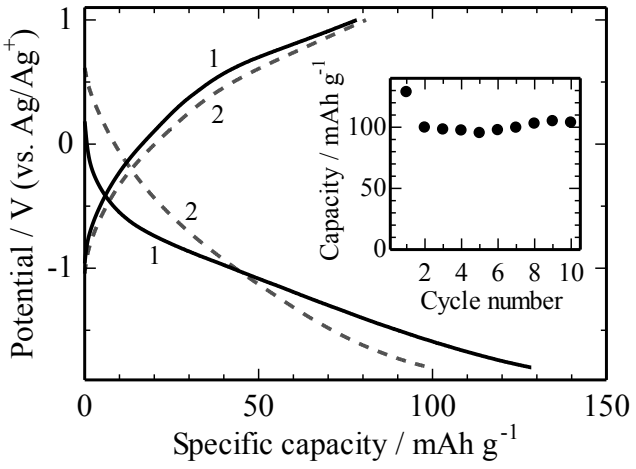

Figure 3. Discharge and charge curves of TodMO at 100-mA g^{-1} current density. The inset shows the discharge capacity observed at various cycles.

degree of crystallinity of the layered manganese oxide is known to affect the morphology of the resultant TodMO [17]. Here, the chemical composition of the obtained TodMO was determined using inductively coupled plasma atomic emission spectroscopy (ICP-AES) measurements and thermogravimetry analysis, yielding $Mg_{0.19}Na_{0.07}MnO_2 \cdot 0.37H_2O$.

Figure 3 shows the discharge and charge curves of the TodMO measured at a current density of 100 mA g^{-1}. The small figures indicate the cycle number. It can be seen that the discharge and charge curves did not exhibit clear plateaus. Further, the separation between the discharge and charge was relatively large, indicating large polarization. The TodMO exhibited a capacity of 130 mAh g^{-1} at the initial discharge; it subsequently exhibited relatively stable capacity at 100 and 80 mAh g^{-1} for discharging and charging, respectively. The inset shows the cycle number dependence of the electrode discharge capacity for the first ten cycles. The Ca/Mn ratios in the electrodes were determined using ICP-AES after the initial discharge and subsequent charging, yielding 21% and 10%, respectively. Hence, a change in composition was observed as a result of the electrochemical reduction/oxidation.

In order to clarify the reaction mechanism in detail, XAS measurements were conducted at the Mn K-edge for the as-prepared TodMO and the electrodes in both the discharged and charged states; the results are shown in Fig. 4. The X-ray absorption near-edge structure (XANES) spectra are related to the structures around the absorbing atoms and their electronic states [18]. When reduction/oxidation reactions occur without a change in structure, as can be seen in the case of the intercalation reaction, the XANES spectra shift to a low energy on reduction, and to a high energy on oxidation without significant shape change. Here, the shape changed slightly after the electrochemical measurements, as can be seen in the XANES spectra shown in Fig. 4(a). This behavior is more obvious for the first derivative of the absorbance shown in Fig. 4(b). This result indicates the structural change from a [3 × 3] tunnel structure and the formation of another compound. The XANES spectrum of the charged state is in good accordance with that of α-

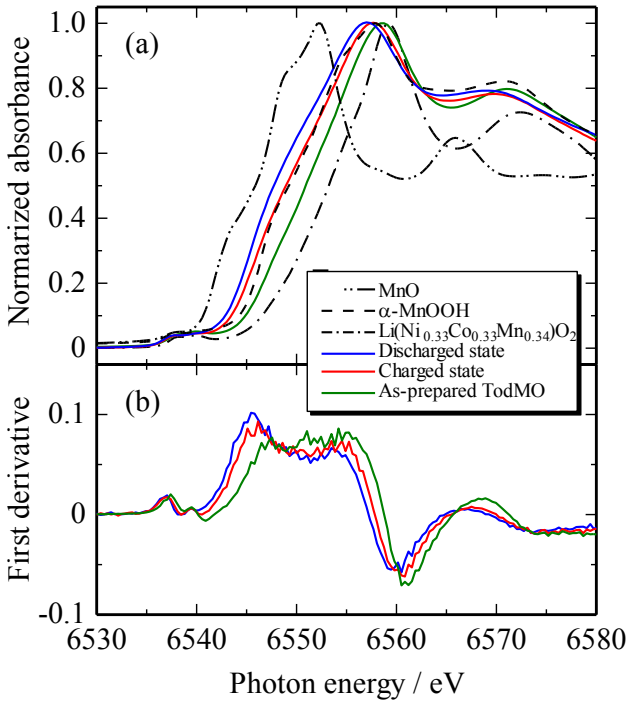

Figure 4. (a) X-ray absorption spectra for TodMO of as-prepared state (black line), discharged state at 3rd cycle (blue line), and charged state at 3rd cycle (red line), measured at Mn K-edge. The reference spectra of MnO (two-dot chain line), α-MnOOH (broken line), and $Li(Ni_{0.33}Co_{0.33}Mn^{+4}_{0.34})O_2$ (chain line) are also shown. (b) First derivatives of the normalized absorbance shown in (a).

MnOOH. Thus, the valence state of Mn in the charged state is Mn^{3+}, and the valence state of Mn in the discharged state is lower than 3+. In order to clarify the reaction of the newly formed Mn^{3+}-compound, electrochemical measurements were performed under two particular conditions, as explained below.

The first examined condition was constant-voltage discharging. An electrode was discharged to −1.8 V at a constant current density of 5 mA g^{-1} and the voltage was then maintained for 24 h. Subsequently, the electrode was charged, but it did not exhibit any charge capacity. The electrode was removed from the cell and analyzed using XAS, at the Mn $L_{2,3}$-edges and without air exposure; the results are shown in Fig. 5. The average valence number of Mn in the zero-capacity electrode was determined to be 2.2, using the MnO and Mn_2O_3 results as the standard samples. Arthur et al. recently reported the formation of Mg-Mn^{2+}-oxide on the surface of hollandite-type manganese oxide with [2 × 2] tunnel structure when the manganese oxide was evaluated as cathodes of Mg batteries [19]. Evaluation of [3 × 3] tunnel-structured manganese oxide as cathodes of Ca batteries also led to the formation of Mn^{2+}-compound. The above results indicate that the electrochemical reduction reaction leads to the formation of two reduction products: electrochemically active manganese oxide and an inactive Mn^{2+} compound.

Further, during sample preparation for the XAS measurements, we found that the electrodes exhibited potential relaxation over 48

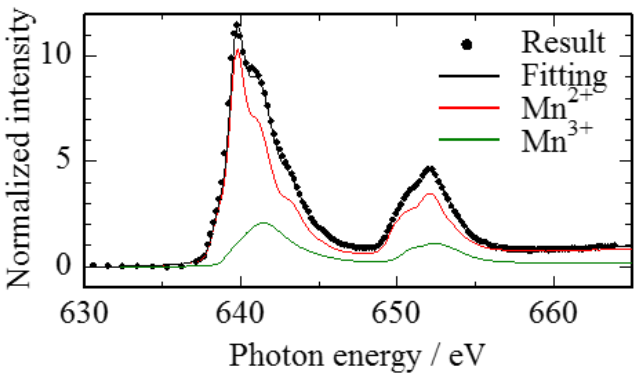

Figure 5. X-ray absorption spectrum of electrode maintained at −1.8 V for 24 h measured in the total electron yield mode at the Mn $L_{2,3}$-edge (solid circles). The black line shows the result of linear combination fitting using the MnO (red line) and Mn_2O_3 (green line) reference spectra.

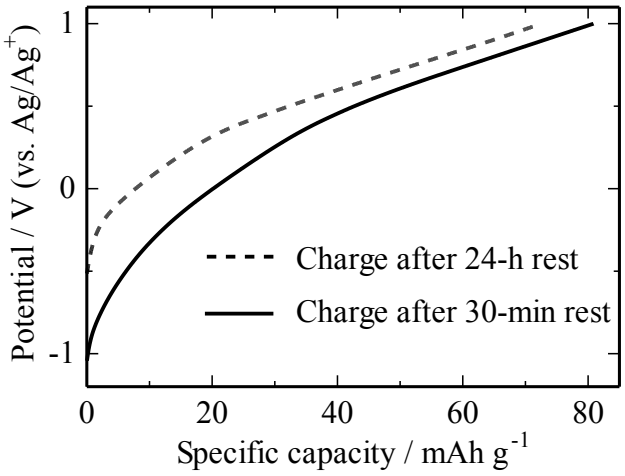

Figure 6. Charge curves after discharging and subsequent rest for 30 min or 24 h.

h after the constant-current discharging and charging had ceased. Thus, we employed discharging and charging after various rest periods as the second particular condition. Figure 6 shows the charge curves of the electrode after discharging followed by rests for 30 min or 24 h. Long rest periods caused fading of the reversible capacity. The measured potentials after the 30-min and 24-h rests were −1.05 and −0.50 V, respectively. The behavior of the charge curves above 0.5 V appears to be similar regardless of the rest time. This result indicates that the electrochemically active reduction product is unstable, and that it converts to the electrochemically inactive phase. The formation of the inactive phase is the cause of the irreversible capacity observed after the second cycle.

The TodMO reaction mechanism is summarized as follows.

(i) TodMO converts to an Mn^{3+} compound with another structure during electrochemical reaction.

(ii) The electrochemical reduction of the newly formed Mn^{3+}-compound leads to the formation of two reduction products: electrochemically active manganese oxide and an inactive Mn^{2+} compound. The electrochemically active reduction product is responsible for the reversible capacity.

(iii) The electrochemically active reduction product is unstable, and it gradually converts to an electrochemically inactive Mn^{2+} compound.

The shape of initial discharge curve is different from those of subsequent discharge curves as shown in Fig. 3. This would be caused by the conversion reaction from TodMO to Mn^{3+} compound.

Despite a todorokite-type manganese oxide with [3 × 3] tunnel structure itself did not act as calcium intercalation host material, the current density of 100 mA g^{-1} employed in this study is relatively large for a battery cathode material in which polyvalent cations are used as carrier ions. The results of this study suggest the feasibility of high-rate-capable cathodes of Ca batteries by making clear the details of the observed reactions.

4. CONCLUSION

The reaction mechanism of todorokite-type manganese oxide (TodMO) in a non-aqueous calcium electrolyte solution has been examined using electrochemical and X-ray absorption spectroscopy measurements, and the following mechanism has been revealed: (i) TodMO converts to an Mn^{3+} compound with another structure during electrochemical reaction; (ii) the newly formed Mn^{3+} compound reacts almost reversibly; and (iii) the discharged state is unstable; and gradually converts to an electrochemically inactive Mn^{2+} compound.

5. ACKNOWLEDGEMENTS

The XAS experiments at Mn K-edge were carried out in KEK-PF under the approval of the PF-PAC (#2007G636). Those at Mn $L_{2,3}$-edge were carried out at SR center of Ritsumeikan University supported by the MEXT Open Advanced Research Facilities Initiative.

REFERENCES

[1] P.G. Bruce, S. A. Freunberger, L. J. Hardwick, J.-M. Tarascon, Nat. Mat., 11, 19 (2012).
[2] F. Cheng, J. Chen, Chem. Soc. Rev., 41, 2172 (2012).
[3] J. Muldoon, C. B. Bucur, T. Gregory, Chem. Rev., 114, 11683 (2014).
[4] D. Aurbach, Z. Lu, A. Schechter, Y. Gofer, H. Gizbar, R. Turgeman, Y. Cohen, M. Moshkovich, E. Levi, Nature, 407, 724 (2000).
[5] E. Levi, Y. Gofer, D. Aurbach, Chem. Mater., 22, 860 (2010).
[6] A. Ponrouch, C. Frontera, F. Bardé, M. R. Palacin, Nat. Mater., 15, 169 (2016).
[7] M.-C. Lin, M. G. Gong, B. Lu, Y. Wu, D.-Y. Wang, M. Guan, M. Angell, C. Chen, J. Yang, B.-J. Hwang, H. Dai, Nature, 520, 324 (2015).
[8] R. Mohtadi, F. Mizuno, J. Nanotechnol., 5, 1291 (2014).

[9] I. Kim, K. Yamabuki, M. Morita, H. Tsutsumi, N. Yoshimoto, J. Power Sources, 278, 340 (2015).
[10]E. Levi, A. Mitelman, D. Aurbach, M. Brunelli, Chem. Mater., 19, 5131 (2007).
[11]S. Rasul, S. Suzuki, S. Yamaguchi, M. Miyayama, Solid State Ionics, 225, 542 (2012).
[12]S. Rasul, S. Suzuki, S. Yamaguchi, M. Miyayama, Electrochem. Acta, 82, 243 (2012).
[13]S. Rasul, S. Suzuki, S. Yamaguchi, M. Miyayama, Electrochim. Acta, 110, 247 (2013).
[14]N. Kumagai, S. Komaba, H. Sakai, H. Sakai, J. Power Sources, 97–98, 515 (2001).
[15]D. Aurbach, R. Skaletsky, Y. Gofer, J. Electrochem. Soc., 138, 3536 (1991).
[16]M. Hayashi, H. Arai, H. Ohtsuka, Y. Sakurai, J. Power Sources, 119–121, 617 (2003).
[17]Z.-H. Liu, L. Kang, K. Ooi, Y. Makita, Q. Feng, J. Colloid Interface Sci., 285, 239 (2005).
[18]N. M. Brown, J. B. McMonegle, G. N. Greves, J. Chem. Soc. Faraday Trans., 80, 589 (1984).
[19]T. S. Arthur, R. Zhang, C. Ling, P.-A. Glans, X. Fan, J. Guo, F. Mizuno, ACS Appl. Mater. Interfaces, 6, 7004 (2014).